The reason why some LAM patients suffer from lymphedema and its mechanism(s) remain unknown. LAM is a neoplastic disease, characterized by both the proliferation of LAM cells and LAM-associated lymphangiogenesis,[17,18] the latter presumably mediated by VEGF-D produced by LAM cells.[19] Serum VEGF-D concentration was reported to be a good biomarker for lymphatic involvement in LAM[20] and indeed, five of eight patients in our study population showed very high serum VEGF-D concentration (>5000 pg/ml). Although the number of LAM patients analyzed here was small, no apparent correlation existed among serum VEGF-D level, extent of lymphangioleiomyomas, and site or stage of lymphedema.

Although the existence of lymphangioleiomyomas does not always lead to a LAM-associated lymphedema in the patient's lower extremities, subclinical dysfunction of axial lymphatics is clearly implied. Actually, the lymphedema around patient #7's left thigh and buttocks could be attributed to the restriction of tight clothing, since loosening her underwear resolved the lymphedema without further treatment. Patient #4 (JUL181) experienced lymphedema around the right buttock and thigh only after an abdominal bandage was applied to gently squeeze out chylous ascites. Even these few cases, though, illustrate the increased amount of subcutaneous lymphatic flow bypassing the usual axial lymphatic route with impaired drainage. Supporting this notion, lymphoscintigraphy clearly delineated a dermal lymphatic flow in patient #5 (JUL213) possibly due to a blockade of lymphatic flow draining into an axial lymphatics in the pelvic cavity from lower extremities by an inguinal lymphangioleiomyoma (Fig. 3). Furthermore, subclinical lymphatic dysfunction has been supported by radiologic findings that the size of lymphagioleiomyomas undergoes dramatic diurnal variation, i.e., enlargement in the afternoon resulting from increased lymphatic flow after physical activity in the morning.[21,22]

Lymphedema is often difficult to treat, particularly if not diagnosed at an early stage.[23] In general, subcutaneous tissue becomes fibrotic and then spreads circumferentially if treatment is not initiated. Eventually, the involved skin becomes hyperkeratotic, hyperpigmented, and papillomatous or verrucous with increased skin turgor.[6] The approach to managing lymphedema is largely dependent upon physiotherapeutic techniques. The term complex decongestive physiotherapy (CDP) refers to an empirically derived, multicomponent program that is designed to reduce the degree of lymphedema and to maintain the health of the skin and supporting structures.[24–26] Some evidence indicates that this approach stimulates lymphatic transport and facilitates the dispersal of retained interstitial proteins. Seven patients reviewed here were treated with both CDP and FRD. Once lymphedema was ameliorated or completely resolved, the condition was sufficiently self-managed by CDP alone except for the four patients (patients #2–#5) with chylous effusions. GnRH therapy was added to the regimen of these four patients, and FRD continued. Although a controversy still existed regarding the effect of hormone therapy (estrogen-depleting treatment) on LAM, we added GnRH therapy to the regimen of these four patients who had chylous effusion to stabilized LAM and ameliorate chylous effusion. For all eight of these patients, lymphedema was mitigated completely or well-controlled with CDP, GnRH therapy, and FRD. An additional possibility comes from recent evidence that sirolimus, a mTOR inhibitor, stabilizes lung function[27] and causes chylous effusion to subside.[28] Similarly, Chachaj et al. reported the successful treatment of lymphedema, chylous ascites, and pleural effusion with sirolimus.[13] However, our combined multimodal approach is likely to be a choice for LAM-associated lymphedema without chylous effusion, particularly when sirolimus treatment is contraindicated.

In conclusion, this is the first review, to our knowledge, of the frequency of LAM-associated lymphedema and its clinical features. In even this small population of LAM patients, lymphedema appears to be a very important presenting feature that signals the possibility of LAM as an underlying disease. The dysfunction of axial lymphatics, undoubtedly caused by proliferation and infiltration of LAM cells along those sites, as well as the high level of serum VEGF-D quantified here are significant factors in the occurrence of lymphedema, but the reason why all LAM patients with these factors do not have lymphedema is unknown. The combined multimodal treatments documented in this analysis were effective for resolving or controlling lymphedema in patients with LAM.

Source of support

This study was supported by a grant to the Respiratory Research Group from the Ministry of Health, Labour and Welfare, Japan; in part by the High Technology Research Center Grant from the Ministry of Education, Culture, Sports, Science, and Technology, Japan; and in part by the Institute for Environmental and Gender-Specific Medicine, Juntendo University, Graduate School of Medicine.

Conflicts of interest statement

None of the authors has any conflicts of interest with regard to this study.

Acknowledgment

We thank Phyllis Minick for excellent assistance in the review of English.

References

1. Carsillo T, Astrinidis A, Henske EP. Mutations in the tuberous sclerosis complex gene TSC2 are a cause of sporadic pulmonary lymphangioleiomyomatosis. *Proc Natl Acad Sci U S A* 2000; **97**(11):6085–90.
2. Sato T, Seyama K, Fujii H, Maruyama H, Setoguchi Y, Iwakami S, et al. Mutation analysis of the TSC1 and TSC2 genes in Japanese patients with pulmonary lymphangioleiomyomatosis. *J Hum Genet* 2002;**47**(1):20–8.
3. Hayashida M, Seyama K, Inoue Y, Fujimoto K, Kubo K. The epidemiology of lymphangioleiomyomatosis in Japan: a nationwide cross-sectional study of presenting features and prognostic factors. *Respirology* 2007;**12**(4):523–30.
4. Kerchner K, Fleischer A, Yosipovitch G. Lower extremity lymphedema update: pathophysiology, diagnosis, and treatment guidelines. *J Am Acad Dermatol* 2008;**59**(2):324–31.

5. Tobin MB, Lacey HJ, Meyer L, Mortimer PS. The psychological morbidity of breast cancer-related arm swelling. Psychological morbidity of lymphoedema. *Cancer* 1993;**72**(11):3248–52.
6. McWayne J, Heiney SP. Psychologic and social sequelae of secondary lymphedema: a review. *Cancer* 2005;**104**(3): 457–66.
7. Makita H, Nasuhara Y, Nagai K, Ito Y, Hasegawa M, Betsuyaku T, et al. Characterization of phenotypes based on severity of emphysema in chronic obstructive pulmonary disease. *Thorax* 2007;**62**(11):932–7.
8. Piller N, Carati C. The diagnosis and treatment of peripheral lymphedema. *Lymphology* 2009;**42**(3):146–7.
9. Ko DS, Lerner R, Klose G, Cosimi AB. Effective treatment of lymphedema of the extremities. *Arch Surg* 1998;**133**(4):452–8.
10. Hayashi T, Koike K, Kumasaka T, Saito T, Mitani K, Terao Y, et al. Uterine angiosarcoma associated with lymphangioleiomyomatosis in a patient with tuberous sclerosis complex: an autopsy case report with immunohistochemical and genetic analysis. *Hum Pathol* 2012;**43**(10):1777–84.
11. Abe R, Kimura M, Airosaki A, Ishii H, Nakamura T, Kasai M, et al. Retroperitioneal lymphangiomyomatosis with lymphedema of the legs. *Lymphology* 1980;**13**(2):62–7.
12. van Lith JM, Hoekstra HJ, Boeve WJ, Weits J. Lymphoedema of the legs as a result of lymphangiomyomatosis. A case report and review of the literature. *Neth J Med* 1989;**34**(5–6):310–6.
13. Chachaj A, Drozdz K, Chabowski M, Dziegiel P, Grzegorek I, Wojnar A, et al. Chyloperitoneum, chylothorax and lower extremity lymphedema in woman with sporadic lymphangioleiomyomatosis successfully treated with sirolimus: a case report. *Lymphology* 2012;**45**(2):53–7.
14. Szuba A, Shin WS, Strauss HW, Rockson S. The third circulation: radionuclide lymphoscintigraphy in the evaluation of lymphedema. *J Nucl Med* 2003;**44**(1):43–57.
15. Szuba A, Cooke JP, Yousuf S, Rockson SG. Decongestive lymphatic therapy for patients with cancer-related or primary lymphedema. *Am J Med* 2000;**109**(4):296–300.
16. Yamamoto R, Yamamoto T. Effectiveness of the treatment-phase of two-phase complex decongestive physiotherapy for the treatment of extremity lymphedema. *Int J Clin Oncol* 2007; **12**(6):463–8.
17. Kumasaka T, Seyama K, Mitani K, Sato T, Souma S, Kondo T, et al. Lymphangiogenesis in lymphangioleiomyomatosis: its implication in the progression of lymphangioleiomyomatosis. *Am J Surg Pathol* 2004;**28**(8):1007–16.
18. Kumasaka T, Seyama K, Mitani K, Souma S, Kashiwagi S, Hebisawa A, et al. Lymphangiogenesis-mediated shedding of LAM cell clusters as a mechanism for dissemination in lymphangioleiomyomatosis. *Am J Surg Pathol* 2005;**29**(10): 1356–66.
19. Seyama K, Kumasaka T, Souma S, Sato T, Kurihara M, Mitani K, et al. Vascular endothelial growth factor-D is increased in serum of patients with lymphangioleiomyomatosis. *Lymphat Res Biol* 2006;**4**(3):143–52.
20. Glasgow CG, Avila NA, Lin JP, Stylianou MP, Moss J. Serum vascular endothelial growth factor-D levels in patients with lymphangioleiomyomatosis reflect lymphatic involvement. *Chest* 2009;**135**(5):1293–300.
21. Avila NA, Bechtle J, Dwyer AJ, Ferrans VJ, Moss J. Lymphangioleiomyomatosis: CT of diurnal variation of lymphangioleiomyomas. *Radiology* 2001;**221**:415–21.
22. Avila NA, Dwyer AJ, Murphy-Johnson DV, Brooks P, Moss J. Sonography of lymphangioleiomyoma in lymphangioleiomyomatosis: demonstration of diurnal variation in lesion size. *AJR Am J Roentgenol* 2005;**184**:459–64.
23. Erickson VS, Pearson ML, Ganz PA, Adams J, Kahn KL. Arm edema in breast cancer patients. *J Natl Cancer Inst* 2001; **93**(2):96–111.
24. Lawenda BD, Mondry TE, Johnstone PA. Lymphedema: a primer on the identification and management of a chronic condition in oncologic treatment. *CA Cancer J Clin* 2009;**59**(1):8–24.
25. Rockson SG. Diagnosis and management of lymphatic vascular disease. *J Am Coll Cardiol* 2008;**52**(10):799–806.
26. Rockson SG. Lymphedema therapy in the vascular anomaly patient: therapeutics for the forgotten circulation. *Lymphat Res Biol* 2005;**3**(4):253–5.
27. McCormack FX, Inoue Y, Moss J, Singer LG, Strange C, Nakata K, et al., National Institutes of Health Rare Lung Diseases Consortium; MILES Trial Group. Efficacy and safety of sirolimus in lymphangioleiomyomatosis. *N Engl J Med* 2011;**364**(17): 1595–606.
28. Taveira-DaSilva AM, Hathaway O, Stylianou M, Moss J. Changes in lung function and chylous effusions in patients with lymphangioleiomyomatosis treated with sirolimus. *Ann Intern Med* 2011;**154**(12):797–805.

J Occup Health 2013; 55: 307–311

Journal of Occupational Health

Brief Report

A Cross-sectional Study of the Association between Working Hours and Sleep Duration among the Japanese Working Population

Tadahiro OHTSU[1], Yoshitaka KANEITA[2], Sayaka ARITAKE[3], Kazuo MISHIMA[4], Makoto UCHIYAMA[5], Tsuneto AKASHIBA[6], Naohisa UCHIMURA[7], Shigeyuki NAKAJI[8], Takeshi MUNEZAWA[9], Akatsuki KOKAZE[1] and Takashi OHIDA[10]

[1]Department of Public Health, Showa University School of Medicine, Japan, [2]Department of Public Health and Epidemiology, Faculty of Medicine, Oita University, Japan, [3]Department of Somnology, Tokyo Medical University, Japan, [4]Department of Psychophysiology, National Institute of Mental Health, National Center of Neurology and Psychiatry, Japan, [5]Department of Psychiatry, Nihon University School of Medicine, Japan, [6]Department of Sleep and Respiratory Medicine, Nihon University School of Medicine, Japan, [7]Department of Neuropsychiatry, Kurume University School of Medicine, Japan, [8]Department of Social Medicine, Hirosaki University Graduate School of Medicine, Japan, [9]ADVANTAGE Risk Management Co., Ltd., Japan and [10]Department of Public Health, Nihon University School of Medicine, Japan

Abstract: A Cross-sectional Study of the Association between Working Hours and Sleep Duration among the Japanese Working Population: Tadahiro OHTSU, *et al.* Department of Public Health, Showa University School of Medicine, Japan—Objectives: This study aimed to clarify the association between long working hours and short sleep duration among Japanese workers. **Methods:** We selected 4,000 households from across Japan by stratified random sampling and conducted an interview survey of a total of 662 participants (372 men; 290 women) in November 2009. Logistic regression analyses were performed using "sleep duration <6 hours per day" as a dependent variable to examine the association between working hours/overtime hours and short sleep duration. **Results:** When male participants who worked for ≥7 but <9 hours per day were used as a reference, the odds ratio (OR) for short sleep duration in those who worked for ≥11 hours was 8.62 (95% confidence interval [CI]: 3.94–18.86). With regard to overtime hours among men, when participants without overtime were used as a reference, the OR for those whose period of overtime was ≥3 hours but <4 hours was 3.59 (95% CI: 1.42–9.08). For both men and women, those with long weekday working hours tended to have a short sleep duration during weekdays and holidays. **Conclusions:** It is essential to avoid working long hours in order to prevent short sleep duration.
(J Occup Health 2013; 55: 307–311)

Key words: Holiday, Overtime hours, Sleep duration, Weekday, Working hours

Received Nov 6, 2012; Accepted Apr 5, 2013
Published online in J-STAGE May 2, 2013
Correspondence to: Y. Kaneita, Department of Public Health and Epidemiology, Faculty of Medicine, Oita University, 1–1 Hasama-machi Idaigaoka, Yufu City, Oita 879-5593, Japan (e-mail: kaneita.yoshitaka@gmail.com)

Van der Hulst reviewed studies published between January 1996 and June 2001 on the association between long working hours and health and identified 6 studies that had used sleep hours as one of the outcome measures[1]. All of those studies had been conducted in Japan; one used a longitudinal design[2], and the others used a cross-sectional design[3–7]. Among them, only one focused on the association between sleep and working hours[7].

In November 2010, Kobayashi *et al.* conducted a systematic review of studies published in 1998 or later on the role played by sleep duration in the association between working hours and cerebrovascular/cardiovascular diseases[8]. They found only two reports on the association between working hours and sleep duration (a cohort study in the UK[9] and a large-scale cross-sectional study in Australia[10]) and recommended further studies on this issue[8].

Here we provide new data regarding the association between long working hours and short sleep duration, although our approach was limited by being a cross-sectional survey with a small sample size.

Materials and Methods

The subjects of this study were selected as follows. A total of 4,000 households were randomly selected across the country, and 2,206 adults were home when the researchers visited the households; 1,224 of them (539 men and 685 women; response rate: 55.5%) agreed to participate in the interview survey[11]. Of these, 662 (372 men; 290 women) were employed, and their data were analyzed. The duration of the survey was 1 month (November 2009). Approval was obtained from the Ethics Committee for Epidemiological Studies of Nihon University School of Medicine before the study began.

The survey included the following items: (1) sex, age, years of schooling completed (junior high/high school/college or university) and size of the city of residence (19 large cities/other cities/towns or villages); (2) working hours and overtime (extra working) hours per weekday; and (3) sleep duration per day on weekdays (workdays) and holidays (Sundays or days off). Regarding (2) and (3), participants were requested to select an answer about their status in the past month from among the categorical answer options provided. We did not ask about work patterns or burden of housework.

In our statistical analyses of working and overtime hours per weekday and sleep duration per day on weekdays and holidays, the composition in each category was calculated based on sex. The univariate logistic regression analyses used "sleep duration <6 hours per day" as a dependent variable and working hours or overtime hours as an explanatory variable and were performed for weekdays and holidays according to sex. Each model was adjusted for age class, years of schooling completed and size of the city of residence. The significance level was set at 5% (two-sided), and the IBM SPSS Statistics 20 software package was used for statistical analysis.

In Japan, overtime is defined as extra working hours that exceed 40 hours per week, excluding breaks, but including working hours on holidays (according to the Ministry of Health, Labour and Welfare integrated measures for prevention of health problems caused by overwork).

Results

Working hours, overtime hours and sleep duration are shown in Table 1 (classified according to sex). A large difference was observed between men and women with regard to working hours and overtime hours per weekday. The proportions of the participants with <6 hours' sleep per day on weekdays and holidays were 34.8% and 16.8%, respectively, among men and 44.3% and 27.0%, respectively, among women. Thus, significant differences were observed between men and women for sleep duration on weekdays and holidays. The average ages (standard deviation) of the men and women were 45.0 (13.7) and 45.3 (12.6) years, respectively, and no significant age-related difference was observed (Mann-Whitney U test; p=0.491).

Table 1. Gender-based working hours, overtime hours and sleep duration

	Men	Women	p value[b]
	n=372[a]	n=290[a]	
Working hours per weekday			<0.001
<5 h	5.1	27.2	
≥5 h, <7 h	10.8	22.6	
≥7 h, <9 h	51.4	36.2	
≥9 h, <11 h	21.9	6.3	
≥11 h	10.8	7.7	
Overtime hours[c] per weekday			<0.001
None	41.3	71.8	
<2 h	30.9	23.2	
≥2 h, <3 h	9.9	2.5	
≥3 h, <4 h	6.6	0.7	
≥4 h	11.3	1.8	
Sleep duration on weekdays[d]			0.002
<6 h	34.8	44.3	
≥6 h, <7 h	40.4	40.8	
≥7 h, <8 h	19.1	13.5	
≥8 h	5.7	1.4	
Sleep duration on holidays[e]			<0.001
<6 h	16.8	27.0	
≥6 h, <7 h	28.4	39.1	
≥7 h, <8 h	33.2	22.8	
≥8 h, <9 h	17.8	6.6	
≥9 h	3.8	4.5	(%)

[a]In each section, the response "I do not know" was excluded from the statistical analyses. [b]χ^2 test. [c]Extra working hours. [d]Workdays. [e]Sundays or days off.

The results of the logistic regression analyses using "sleep duration <6 hours per day" as a dependent variable are shown in Table 2. When participants working ≥7 but <9 hours per day were used as a reference, the odds ratio (OR) for "sleep duration <6 hours per day" on weekdays was significantly higher among those working ≥9 hours per weekday. In the same group of participants, the OR for holidays was also significantly high. With regard to overtime hours, when participants without overtime were used as a reference, the OR for having "sleep duration <6 hours per day" on

Table 2. Logistic regression analyses using "sleep duration <6 hours per day" as a dependent variable[a]

	Sleep duration on weekdays[b]				Sleep duration on holidays[c]			
Explanatory variables	n[d]	AOR	95% CI	*p* value	n[d]	AOR	95% CI	*p* value
Men								
Working hours per weekday								
<7 h	58	1.67	0.83–3.36	0.152	57	3.69	1.59–8.55	0.002
≥7 h, <9 h	190	1.00	Reference		190	1.00	Reference	
≥9 h, <11 h	81	2.76	1.57–4.86	<0.001	81	2.71	1.27–5.79	0.010
≥11 h	40	8.62	3.94–18.86	<0.001	40	5.59	2.43–12.86	<0.001
Overtime hours[e] per weekday								
None	150	1.00	Reference		150	1.00	Reference	
<2 h	111	0.91	0.52–1.62	0.757	111	0.55	0.25–1.18	0.123
≥2 h, <3 h	36	1.05	0.46–2.37	0.912	35	0.28	0.06–1.28	0.101
≥3 h, <4 h	24	3.59	1.42–9.08	0.007	24	2.02	0.73–5.62	0.179
≥4 h	41	3.46	1.64–7.30	0.001	41	1.45	0.62–3.41	0.396
Women								
Working hours per weekday								
<5 h	78	1.13	0.60–2.10	0.709	78	1.45	0.71–2.94	0.308
≥5 h, <7 h	65	1.58	0.83–3.03	0.167	65	1.46	0.70–3.06	0.318
≥7 h, <9 h	104	1.00	Reference		104	1.00	Reference	
≥9 h	40	2.51	1.17–5.39	0.018	40	2.23	0.97–5.12	0.060
Overtime hours[e] per weekday								
None	203	1.00	Reference		203	1.00	Reference	
<2 h	66	1.58	0.88–2.82	0.125	66	1.31	0.69–2.49	0.417
≥2 h	14	0.68	0.21–2.20	0.520	14	0.71	0.18–2.76	0.620

[a]Working hours and overtime hours were used as explanatory variables (univariate analysis). Each model was adjusted for age class, years of schooling completed and size of the city of residence. [b]Workdays. [c]Sundays or days off. [d]In each section, the response "I do not know" was excluded from the statistical analyses. [e]Extra working hours. AOR, adjusted odds ratio; CI, confidence interval.

weekdays was 3.59 (95% confidence interval [CI]: 1.42–9.08) among those working ≥3 but <4 hours overtime and 3.46 (95% CI: 1.64–7.30) among those working ≥4 hours overtime, indicating significantly high ORs. No significant OR was observed regarding holidays. Among women, the OR for "sleep duration <6 hours per day" on weekdays was significantly higher among those working ≥9 hours per day and that for holidays among the same group was 2.23 (95% CI: 0.97–5.12). There was no significant OR with regard to overtime hours.

Discussion

The results of this study show that the OR for "sleep duration <6 hours per day" was significantly higher among men working ≥9 hours per day or ≥3 hours overtime. The overall total of overtime was equivalent to >60 hours per month. In Japan, an amendment to the relevant law in 2005 made it obligatory for overworked workers to receive health guidance via an interview with a physician[12]. According to this legislation, 80 hours overtime per month (approximately 4 hours overtime per day) would prevent workers from sleeping the required total of approximately 6 hours per day[13]. The results of our study suggest a need to review this claim and are therefore noteworthy. Kageyama and colleagues reported a significant negative association between ≥60 hours overtime per month in the previous 3 months and sleep length on weekdays among Japanese white-collar workers[7].

Almost half of the women in this study worked <7 hours per day, and most appeared to be part-time workers. For this group of women, the OR for having "<6 hours sleep" was high among those working ≥9 hours, as seen in men. In addition, although more than 70% of women did not work overtime, the proportions of those with <6 hours sleep on weekdays and holidays were higher than in men. The burden of doing housework in addition to employed work may explain this result. From our results, it is unclear to

what extent long working hours were associated with short sleep duration among women.

A cohort study conducted in the UK reported that the OR for short sleep duration (<7 hours) was 3.24 (95% CI: 1.45–7.27) among subjects working >55 hours per week when those with 35–40 working hours per week were used as a reference[9]. In addition, large-scale cross-sectional studies conducted in Australia[10] and the USA[14] indicated that short sleep duration was associated with working long hours. The findings of these overseas studies appear to support our results, although the classifications of working hours and sleep duration differed.

In the present study, both men and women with long weekday working hours tended to have a short sleep duration (<6 hours) on weekdays as well as holidays. Two possible explanations for this are (1) that people working long hours on weekdays spend holidays attending to personal matters that cannot be taken care of on weekdays and (2) that they became accustomed to a short sleep duration. Kageyama and colleagues reported that the amount of overtime was positively correlated with the amount of time spent sleeping on the nights before holidays[4]; however, a later report stated that sleep length before holidays was inversely correlated with overtime[7]. This latter result concurs with that of our study.

This study had some limitations. First, the response rate was not particularly high (55.5%). It is possible that only respondents with enough spare time tended to participate in this survey. Thus, working hours may have been underestimated. In addition, as the ORs in Table 2 for both male and female participants working <7 hours per day were >1, selection bias caused by the low response rate would have led to underestimation of the present findings. Second, the types of jobs varied, and we did not investigate items that might have affected sleep duration, such as presence/absence of shift work, commuting time and family composition. Third, questions on whether participants worked full-time or part-time and had housework burdens such as child-rearing and nursing care were not asked; these issues are particularly relevant to women. Belenky and colleagues stated in a recent report that occupational sleep medicine is a new field within sleep medicine[15]. We hope to design a survey investigating sleep problems in terms of occupational health, in which the aforementioned limitations will be corrected.

This study examined the associations between working hours and sleep duration. Long working hours were associated with short sleep duration (<6 hours). In men, the OR for short sleep duration was significantly higher among participants with ≥3 hours of overtime per day. In addition, sleep duration was short on weekdays as well as on holidays among people with long working hours. It is essential to avoid working long hours in order to prevent short sleep duration.

Acknowledgments: This study was supported by a Health Science Research Grant from the Japanese Ministry of Health, Labour and Welfare (*H20-Junkankitou-Ippan-002*). The authors are very grateful to Dr. Hideyasu Aoyama, professor emeritus at Okayama University, for providing us with strong motivation while developing this report.

References

1) van der Hulst M. Long workhours and health. Scand J Work Environ Health 2003; 29: 171–88.
2) Nakanishi N, Nakamura K, Ichikawa S, Suzuki K, Tatara K. Lifestyle and the development of hypertension: a 3-year follow-up study of middle-aged Japanese male office workers. Occup Med 1999; 49: 109–14.
3) Hayashi T, Kobayashi Y, Yamaoka K, Yano E. Effect of overtime work on 24-hour ambulatory blood pressure. J Occup Environ Med 1996; 38: 1007–11.
4) Kageyama T, Nishikido N, Kobayashi T, Kurokawa Y, Kaneko T, Kabuto M. Long commuting time, extensive overtime, and sympathodominant state assessed in terms of short-term heart rate variability among male white-collar workers in the Tokyo megalopolis. Ind Health 1998; 36: 209–17.
5) Sasaki T, Iwasaki K, Oka T, et al. Effect of working hours on cardiovascular-autonomic nervous functions in engineers in an electronics manufacturing company. Ind Health 1999; 37: 55–61.
6) Sasaki T, Iwasaki K, Oka T, Hisanaga N. Association of working hours with biological indices related to the cardiovascular system among engineers in a machinery manufacturing company. Ind Health 1999; 37: 457–63.
7) Kageyama T, Nishikido N, Kobayashi T, Kawagoe H. Estimated sleep debt and work stress in Japanese white-collar workers. Psychiatry Clin Neurosci 2001; 55: 217–9.
8) Kobayashi T, Takao S, Doi H. Review of the literature on the role of sleep duration in the association between working hours and cerebrovascular/cardiovascular diseases. Occupational Health Journal 2011; 34: 66–71 (in Japanese).
9) Virtanen M, Ferrie JE, Gimeno D, et al. Long working hours and sleep disturbances: the Whitehall II prospective cohort study. Sleep 2009; 32: 737–45.
10) Magee CA, Iverson DC, Caputi P. Factors associated with short and long sleep. Prev Med 2009; 49: 461–7.
11) Ohtsu T, Kaneita Y, Aritake S, et al. Preferable forms of relaxation for health promotion, and the association between recreational activities and self-perceived health. Acta Med Okayama 2012; 66: 41–51.

12) Iwasaki K, Takahashi M, Nakata A. Health problems due to long working hours in Japan: working hours, worker's compensation (*Karoshi*), and preventive measures. Ind Health 2006; 44: 537–40.
13) Wada O. Occupational and life-style risk factors and prevention of "*Karoshi*". Occupational Health Review 2002; 14: 183–213 (in Japanese).
14) Krueger PM, Friedman EM. Sleep duration in the United States: a cross-sectional population-based study. Am J Epidemiol 2009; 169: 1052–63.
15) Belenky G, Wu LJ, Jackson ML. Occupational sleep medicine: practice and promise. Prog Brain Res 2011; 190: 189–203.

PLOS | ONE

An Integrated Expression Profiling Reveals Target Genes of TGF-β and TNF-α Possibly Mediated by MicroRNAs in Lung Cancer Cells

Akira Saito[1,2]*, Hiroshi I. Suzuki[3], Masafumi Horie[1], Mitsuhiro Ohshima[4], Yasuyuki Morishita[3], Yoshimitsu Abiko[5], Takahide Nagase[1]

1 Department of Respiratory Medicine, Graduate School of Medicine, The University of Tokyo, Bunkyo-ku, Tokyo, Japan, **2** Division for Health Service Promotion, The University of Tokyo, Bunkyo-ku, Tokyo, Japan, **3** Department of Molecular Pathology, Graduate School of Medicine, The University of Tokyo, Bunkyo-ku, Tokyo, Japan, **4** Department of Biochemistry, Ohu University School of Pharmaceutical Sciences, Tomitamachi, Koriyama, Fukushima, Japan, **5** Department of Biochemistry and Molecular Biology, Nihon University School of Dentistry at Matsudo, Matsudo, Chiba, Japan

Abstract

EMT (epithelial-mesenchymal transition) is crucial for cancer cells to acquire invasive phenotypes. In A549 lung adenocarcinoma cells, TGF-β elicited EMT in Smad-dependent manner and TNF-α accelerated this process, as confirmed by cell morphology, expression of EMT markers, capacity of gelatin lysis and cell invasion. TNF-α stimulated the phosphorylation of Smad2 linker region, and this effect was attenuated by inhibiting MEK or JNK pathway. Comprehensive expression analysis unraveled genes differentially regulated by TGF-β and TNF-α, such as cytokines, chemokines, growth factors and ECM (extracellular matrices), suggesting the drastic change in autocrine/paracrine signals as well as cell-to-ECM interactions. Integrated analysis of microRNA signature enabled us to identify a subset of genes, potentially regulated by microRNAs. Among them, we confirmed TGF-β-mediated induction of miR-23a in lung epithelial cell lines, target genes of which were further identified by gene expression profiling. Combined with in silico approaches, we determined HMGN2 as a downstream target of miR-23a. These findings provide a line of evidence that the effects of TGF-β and TNF-α were partially mediated by microRNAs, and shed light on the complexity of molecular events elicited by TGF-β and TNF-α.

Citation: Saito A, Suzuki HI, Horie M, Ohshima M, Morishita Y, et al. (2013) An Integrated Expression Profiling Reveals Target Genes of TGF-β and TNF-α Possibly Mediated by MicroRNAs in Lung Cancer Cells. PLoS ONE 8(2): e56587. doi:10.1371/journal.pone.0056587

Editor: Vladimir V. Kalinichenko, Cincinnati Children's Hospital Medical Center, United States of America

Received August 30, 2012; **Accepted** January 11, 2013; **Published** February 20, 2013

Funding: This work was supported by KAKENHI (Grants-in-Aid for Scientific Research) from the Ministry of Education, Culture, Sports, Science, and Technology and grants from the Ministry of Health, Labour and Welfare of Japan. The funders had no role in study design, data collection and analysis, decision to publish, or preparation of the manuscript.

Competing Interests: The authors have declared that no competing interests exist.

* E-mail: asaitou-tky@umin.ac.jp

Introduction

Lung cancer is the most frequent cancer type, which causes death of more than one million people every year. Understanding of molecular events which govern invasive/metastatic spread of cancer cells is crucial for developing novel therapeutics of lung cancer. Epithelial-mesenchymal transition (EMT) is the differentiation switch directing epithelial cells to acquire mesenchymal phenotypes, which plays key roles during embryonic development as well as cancer invasion/metastasis. The hallmark of EMT is E-cadherin downregulation and subsequent loss of cell-cell adhesions, which is coupled with increased expression of mesenchymal markers including N-cadherin and vimentin. Additionally EMT is accompanied with cell morphological changes from 'cuboidal' to 'spindle-like' appearances, which correspond to actin reorganization and cytoskeltal alterations, leading to acquisition of the fibroblast-like migratory phenotype [1], [2].

Transforming growth factor (TGF)-β plays a central role in the regulation of EMT and exhibits its pleiotropic effects through binding to receptors type I (TβR-I) and type II (TβR-II). Upon ligand-induced heteromeric complex formation between TβR-I and TβR-II, TβR-I is phosphorylated by TβR-II and mediates specific intracellular signaling through phosphorylation of receptor-regulated Smads (R-Smads: Smad2 and Smad3 for TGF-β). Phosphorylated R-Smads interact with Smad4 and translocate into the nucleus, where they regulate transcription of target genes [3], [4]. TGF-β is often overexpressed in tumor tissues, and facilitates cancer progression through a diverse repertoire of tumor-cell-autonomous and host–tumor interactions, including enhancement of cell motility and invasion, which involves the process of EMT [5].

Accumulating evidence unravels the molecular mechanisms by which inflammatory responses promote tumor progression [6]. Tumor necrosis factor (TNF)-α is one of the most potent pro-inflammatory cytokines produced in the tumor microenvironment. Upon stimulation, activated IKK (IκB kinase) phosphorylates NFκB inhibitor (IκB) and triggers its rapid degradation through proteasome proteolysis, resulting in the liberation of NFκB, which then translocates to the nucleus and induces a myriad of gene expression involved in immune response [7]. The contribution of NFκB signaling to the initiation and progression of cancer is clearly documented, and several lines of evidence demonstrate that TNF-α and/or NFκB signaling plays a key role in the regulation of EMT [8], [9], [10].

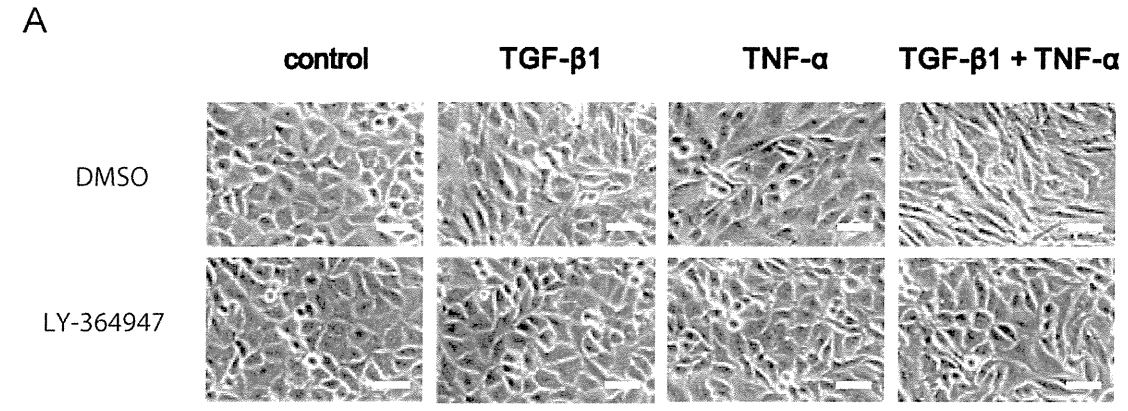
A
control
TGF-β1
TNF-α
TGF-β1 + TNF-α
DMSO
LY-364947

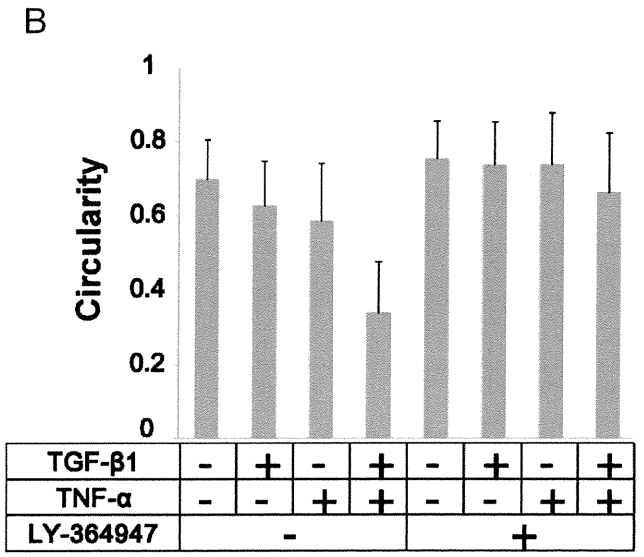
B
Circularity
1
0.8
0.6
0.4
0.2
0
TGF-β1 - + - + - + - +
TNF-α - - + + - - + +
LY-364947 - +

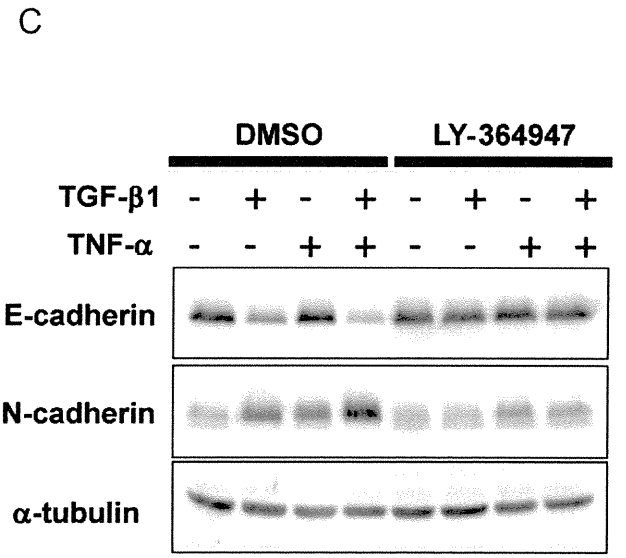
C
DMSO
LY-364947
TGF-β1 - + - + - + - +
TNF-α - - + + - - + +
E-cadherin
N-cadherin
α-tubulin

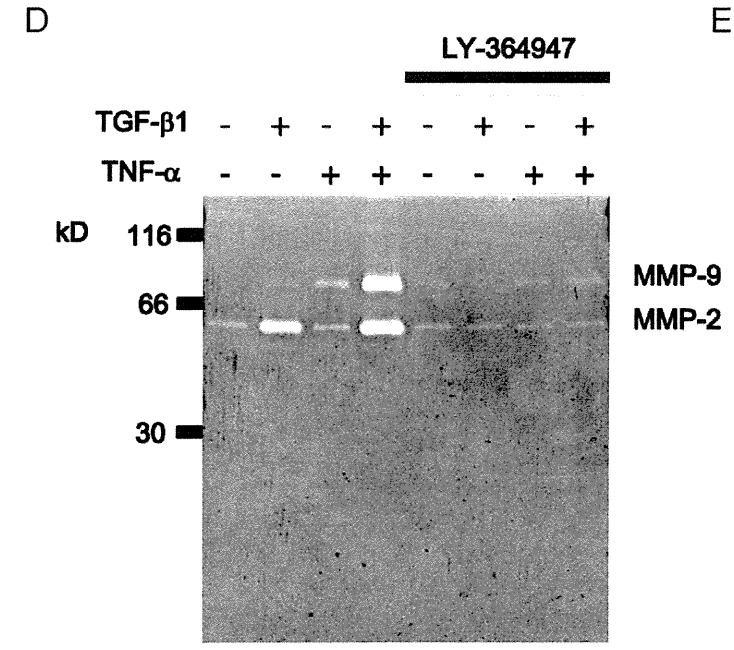
D
LY-364947
TGF-β1 - + - + - + - +
TNF-α - - + + - - + +
kD
116
66
30
MMP-9
MMP-2

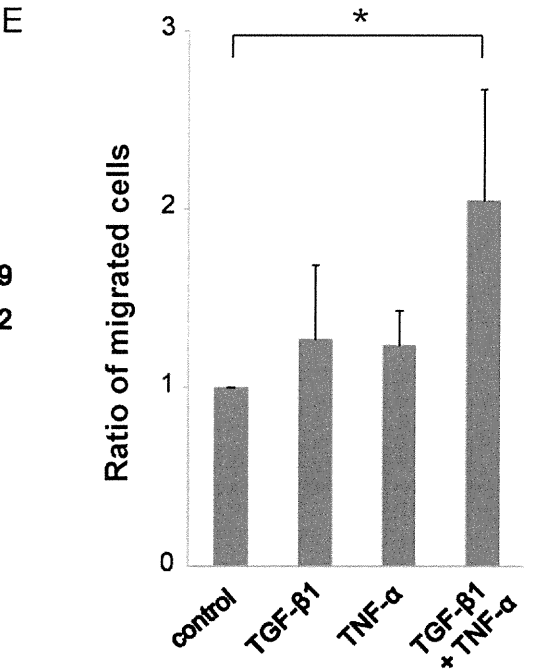
E
*
Ratio of migrated cells
3
2
1
0
control
TGF-β1
TNF-α
TGF-β1 + TNF-α

Figure 1. TNF-α enhances TGF-β-mediated EMT in A549 lung cancer cells. (A) A549 cells were pretreated with LY-364947 (TβR-I inhibitor) or control DMSO for 60 min, further cultured with 5 ng/ml TGF-β1 and/or 10 ng/ml TNF-α for 48 h, and analyzed by phase-contrast microscopy. Bar: 50 μm. (B) Cell circularity was measured using Image J software to quantify cell morphological change following the described treatment. (C) Immunoblotting analyses of E-cadherin and N-cadherin in A549 cells stimulated with TGF-β1 and/or TNF-α for 48 h in the presence or absence of LY-364947. α-tubulin was used as loading control. (D) Gelatin zymography. A549 cells treated as described were cultured with serum free media for additional 48 h. The conditioned media were collected and the same amount of protein was electrophoresed. Gelatin digestion by activated MMP-2 and MMP-9 was visualized by Coomassie blue staining. (E) Cell invasion assay. The migrated cells through the culture inserts coated with Matrigel were trypsinized and counted. Each experiment was performed in triplicate and the averaged relative ratios from 3 independent experiments were presented. Error bars: SD. *$P<0.05$ (Student's t-test).
doi:10.1371/journal.pone.0056587.g001

Noncoding microRNAs (miRNAs) attract increasing attention as key components of cell signaling, which regulate expression levels of multiple proteins, primarily by binding to the 3′ untranslated region (UTR) of targets. Important roles for miRNAs have been shown in tumor progression by modulation of cell differentiation, proliferation, invasion, and metastasis. MicroRNA-200 (miR-200) and miR-205 are critically involved in maintaining the epithelial cell phenotype and are suppressed by TGF-β [11]. It is also reported that miR-21 and miR-31 are synergically induced by TGF-β and TNF-α, which facilitate cancer cell invasion [12].

Recent studies have shown that TNF-α enhances TGF-β-mediated EMT in lung cancer/epithelial cells [13], [14], [15], suggesting the potential crosstalks between these signals. However, little is known about the molecular events how these signals are orchestrated to modulate EMT. We have previously demonstrated that TGF-β induces EMT in A549 lung adenocarcinoma cells [16], which harbor an activating K-ras mutation and form a tumor with well-differentiated adenocarcinoma histology when subcutaneously injected into immunocompromized mice [17], [18]. In the present study, we explored the underlying mechanisms of EMT mediated by TGF-β and TNF-α in A549 cells. In search of the target genes and miRNAs, we performed comprehensive expression analyses in combination with in silico screening. These data delineated subsets of genes differentially or cooperatively regulated by TGF-β and TNF-α, and identified miR-23a as a miRNA target of TGF-β. These analyses further implied the possibility that a subset of TGF-β target genes could be regulated by miRNAs, shedding light on the complexity of molecular events elicited by TGF-β and TNF-α in lung cancer cells.

Materials and Methods

Reagents and Antibodies

TGF-β1 and TNF-α were purchased from Sigma-Aldrich (St. Louis, MO) and R&D Systems (Minneapolis, MN), and were used at the concentration of 5 ng/ml and 10 ng/ml, respectively. Anti-Smad2, phosphorylated (phospho-) Smad2 at Ser 245/250/255, phospho-Smad2 at Ser 465/467, Smad3, phospho-Smad3 at Ser 423/425, Smad4, Erk, phospho-Erk, p38, phospho-p38, phospho-c-Jun and E-cadherin antibodies were from Cell Signaling (Beverly, MA). Anti-N-cadherin antibody was from BD Pharmingen (Transduction Laboratories, Lexington, KY). Anti-α-tubulin antibody was from Sigma-Aldrich. Anti-HMGN2 antibody was from Millipore (Darmstadt, Germany). LY-364947 (TβR-I inhibitor) was used at the concentration of 3 μM. U0126 (MEK 1/2 inhibitor), SP600125 (JNK inhibitor) and SB203580 (p38 inhibitor) were used at the concentration of 25 μM.

Cell Culture

A549 lung adenocarcinoma cells [19] were gifted from Cell Resource Center for Biomedical Research, Institute of Development, Aging and Cancer, Tohoku University (Sendai, Japan). NCI-H441 (H441) lung adenocarcinoma cells and HEK293T cells were from American Type Culture Collection. Transformed human bronchial epithelial cells (BEAS2B cells) were purchased from Summit Pharmaceuticals International (Tokyo, Japan). Cells were photographed using a phase-contrast microscope (Olympus, Tokyo, Japan). Cell circularity was measured by NIH Image J software.

Transfection

Lipofectamine RNAiMAX reagent (Invitrogen) was used for siRNA transfection into A549 cells, and final concentration of siRNA was 20 nM. Human Smad4 siRNA (Stealth RNAi VHS41118) and negative control siRNA were purchased from Invitrogen. The transfected cells were cultured for 48 h and seeded at the same cell density, followed by incubation with TGF-β1 and/or TNF-α. To assess the effect of miR-23a, 10 nM of synthetic precursor miR-23a (pre-miR-23a) or Cy3-labelled negative control (Applied Biosystems, Carlsbad, CA) was transfected into A549 cells using Lipofectamine RNAiMAX reagent. The transfection efficiency judged by Cy3 fluorescence was more than 95% as confirmed by flow cytometry. For microarray analysis, RNA sample was collected 48 h after transfection.

Immunoblot Analysis

Cells were put on ice and rinsed with PBS, then lysed in lysis buffer (20 mM Tris-HCl, pH 7.5, 150 mM NaCl, 1 mM EDTA, 0.5% Nonidet P-40) supplemented with protease and phosphatase inhibitors for immunoblotting. Following centrifugation at 15000 rpm for 15 min, cell lysates were quantitated for protein content by BCA Protein Assay Kit (Pierce, Rockford, IL) and equal amounts of total proteins were processed to SDS-PAGE, followed by semi-dry transfer of the proteins to nitrocellulose membrane. Non-specific binding of proteins to the membrane was blocked by incubation with Amersham ECL Prime Blocking Agent (GE Healthcare, Buckinghamshire, UK) in TBS-T buffer (50 mM Tris-HCl, pH 7.4, 150 mM NaCl, 0.05% Tween-20). The immunoblotted proteins were detected with the ECL blotting system and LightCapture/Ez-Capture imaging system (ATTO, Tokyo, Japan).

RNA Isolation and RT-PCR

Total RNA was isolated using the RNeasy Mini Kit (Qiagen, Hilden, Germany). The synthesis of cDNA was performed using SuperScript III First-Strand Synthesis System (Invitrogen, Carlsbad, CA), according to the manufacturer's instructions. Quantitative RT-PCR analysis was performed using Mx-3000P (Stratagene, La Jolla, CA) and QuantiTect SYBR Green PCR (Qiagen). Expression level was normalized to that of glyceraldehyde-3-phosphate dehydrogenase (*GAPDH*). Primer sequences are shown in Table S1. MicroRNA was isolated using the miRNeasy Mini Kit (Qiagen). Mature miR-23a was reverse-transcribed, and quantitative PCR was performed using TaqMan microRNA assays (Applied Biosystems). Expression level was normalized to that of U6.

A

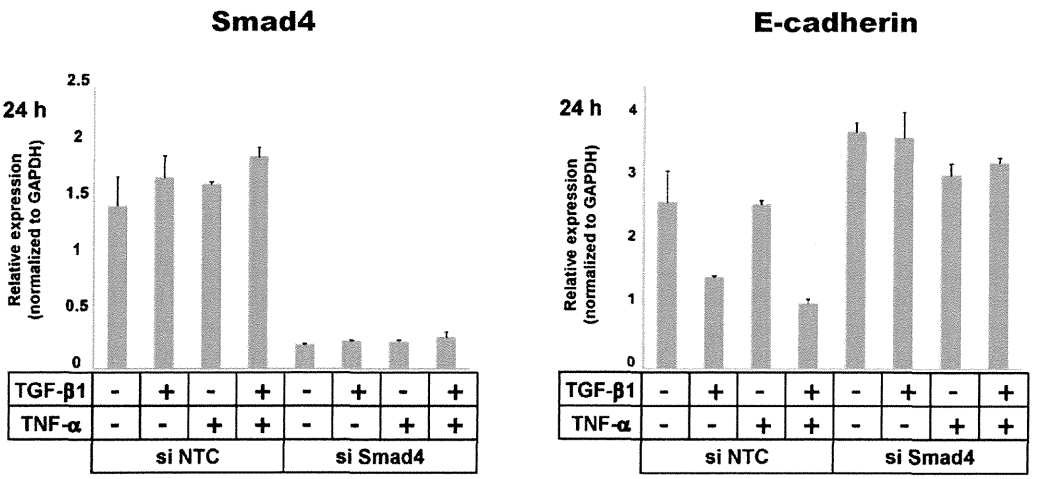
Smad4
E-cadherin
24 h
Relative expression (normalized to GAPDH)
TGF-β1
TNF-α
si NTC
si Smad4

B

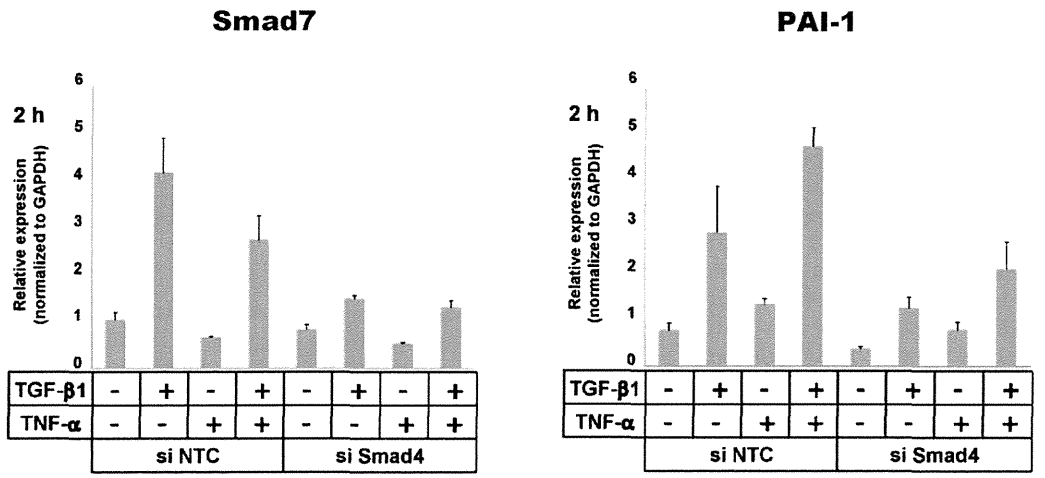
Smad7
PAI-1
2 h
Relative expression (normalized to GAPDH)
TGF-β1
TNF-α
si NTC
si Smad4

C

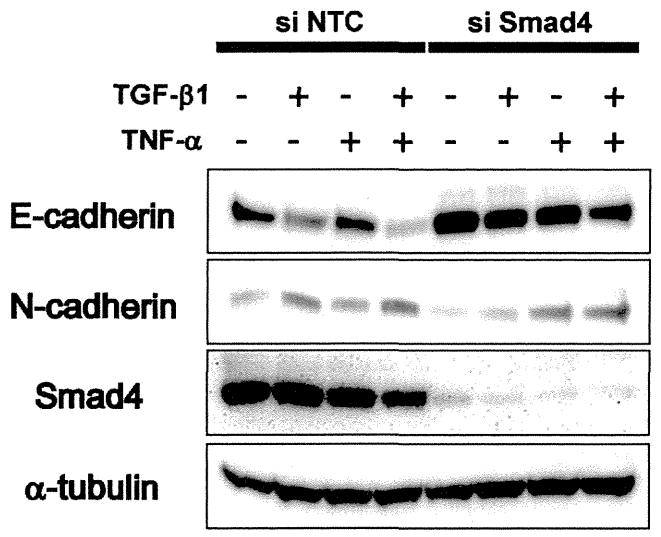
si NTC
si Smad4
TGF-β1
TNF-α
E-cadherin
N-cadherin
Smad4
α-tubulin

Figure 2. TGF-β-mediated EMT is Smad-dependent. (A–B) A549 cells were transfected with siRNAs for Smad4 (si Smad4), or negative control siRNAs (si NTC) and cultured for 48 h. The cells were further cultured with 5 ng/ml TGF-β1 and/or 10 ng/ml TNF-α for 2 h (B) or 24 h (A), and RNA was collected. Quantitative PCR was performed for Smad4, E-cadherin, Smad7 and PAI-1 at the indicated time. Expression was normalized to that of GAPDH. Error bars: SD. (C) Cell lysates were collected 48 h after TGF-β1 and/or TNF-α treatment. Immunoblotting was performed for E-cadherin, N-cadherin and Smad4. α-tubulin was used as loading control.
doi:10.1371/journal.pone.0056587.g002

Gelatin Zymography

Conditioned media without FBS were collected and equal amounts of protein were mixed with 4 × non-reducing SDS-PAGE sample buffer. The samples were applied to a 10% (w/v) polyacrylamide gel impregnated with 1 mg/ml gelatin (Sigma-Aldrich). After electrophoresis, SDS was removed from the gel by washing 3 times for 20 min in 2.5% Triton X-100 solution. Then the gels were incubated overnight with gentle shaking at 37°C in buffer (50 mM Tris-HCl, pH 7.6, 5 mM $CaCl_2$, 200 mM NaCl, 0.02% Brij35). The gel was stained with 0.5% Coomassie blue R250 in 50% methanol and 5% acetic acid for 2 h at room temperature, and subsequently destained with 40% methanol-10% acetic acid solution until the bands became clear.

Invasion Assay

Cell invasion assay was performed using cell culture Inserts with 8 μm pore size (BD Biosciences, Franklin Lakes, NJ). The upper surface of the chamber was coated with growth factor reduced Matrigel (BD Biosciences). A549 cells (4×10^5 cells/well) resuspended in serum free media were seeded in the upper side of the chamber. In the lower side of the chamber, the growth medium supplemented with 10% FBS was added. TGF-β1 and/or TNF-α were added into both sides of the chamber. After 24 h, cells on the lower surface of the chamber were trypsinized, resuspended in PBS and counted with a hemocytometer. The experiments were performed with triplicate, and repeated 3 times. The data are presented as the mean of the ratio compared to control, out of 3 independent experiments.

Expression Profiling

Gene expression profiling was performed using a GeneChip® Human Gene 1.0 ST Array (Affymetrix, Santa Clara, CA). The microarray processing was carried out according to the manufacturer's instructions. The expression of 19,734 genes was monitored, and the data was imported into GeneSpring GX software (Agilent Technologies, Santa Clara, CA) for the selection of induced and repressed genes.

The expression of 1223 mature microRNAs was profiled using Exiqon's miRCURY LNA Array, 6th generation (Filgen, Nagoya, Japan). Briefly, RNA samples were checked for RNA integrity on Bioanalyzer 2100 (Agilent Technologies, Wilmington, DE), labeled with Hy3, and hybridized. Slides were scanned using GenePix®4000B (Molecular Devices, Union City, CA), and the images were digitized with Array-Pro Analyzer Ver. 4.5 (Media Cybernetic, Silver Spring, MD). Finally, data were normalized and expressed as fold increase with the MicroArray Data Analysis Tool Ver. 3.2 (Filgen).

Ingenuity Pathways Analysis (IPA) (Ingenuity Systems, Mountain View, CA) was used for the mapping of gene expression data into relevant pathways based on the gene's functional annotation and known molecular interactions. For integrated analysis of miRNA and mRNA signatures, the miRNA Target Filter in IPA was employed, which extracted possible miRNA-mRNA interactions based on the databases such as TarBase, miRecords and TargetScan.

Luciferase Reporter Assay

Pri-miR23a expression vector was generated by cloning the short fragment of pri-miRNA containing pre-miRNA and flanking sequence into pcDNA6.2-GW/EmGFP-miR (Invitrogen). For the reporter construct, the 3′UTR segment of human HMGN2 gene was cloned into the luciferase reporter vector. The primer sequences used are given in Table S2. HEK293T cells were transfected with each reporter construct with or without pri-miR23a expression vector using FuGENE6 (Roche, Basel, Switzerland). The ratio of renilla to firefly luciferase was measured using the Dual-Luciferase Reporter Assay System (Promega, Madison, WI).

Results

TNF-α Enhances TGF-β-mediated EMT in A549 Lung Cancer Cells

First we characterized the effect of TGF-β and/or TNF-α on EMT in A549 lung cancer cells. At confluency, A549 cells displayed cobblestone-like appearances and TGF-β treatment led to cell morphological change to elongated shape. TNF-α was also potent in inducing cell morphological change to spindle-like appearances. As previously reported, costimulation of TGF-β and TNF-α resulted in dramatic change of cell shape to fibroblast-like appearances [14], which was clearly distinguishable from those observed in the cells treated with TGF-β or TNF-α alone (Figure 1A, upper panels).

Next we examined the effect of the TβR-I kinase inhibitor, LY-364947. Blockade of endogenous TGF-β signaling by LY-364947 resulted in uniformly cuboidal cell morphology, and the effect of exogenous TGF-β was clearly abrogated in the presence of LY-364947. On the other hand, TNF-α-mediated cell morphological change was still observed, albeit to a lesser extent, in the cells pretreated with LY-364947, indicative of the effect of TNF-α alone exerted in the absence of endogenous TGF-β signaling (Figure 1A, lower panels).

These morphological changes were quantified by measuring the cell circularity (Figure 1B). In the cells costimulated with TGF-β and TNF-α, cell circularity was markedly reduced, suggesting the synergic effect on cell morphology. In the presence of LY-364947, their effects were mostly inhibited, implying the critical contribution of TGF-β to the observed synergic effect.

The process of EMT is accompanied by downregulation of E-cadherin and upregulation of N-cadherin, which is termed as cadherin switch [1], [2]. In the following experiments, we examined the expression of E-cadherin and N-cadherin, as epithelial and mesenchymal markers, respectively. E-cadherin expression was mostly abrogated by TGF-β treatment whereas TNF-α alone displayed a marginal effect on E-cadherin downregulation at protein level (Figure 1C). Consistent with the change in E-cadherin expression, N-cadherin was upregulated by treatment with TGF-β or TNF-α. Furthermore, in accordance with the dramatic change in cell morphology, TNF-α enhanced the effect of TGF-β on epithelial/mesenchymal markers. The effect of TGF-β on the expression of E-cadherin/N-cadherin was inhibited by LY-364947 whereas TNF-α-mediated upregulation of N-cadherin was also observed regardless of LY-364947 treatment.

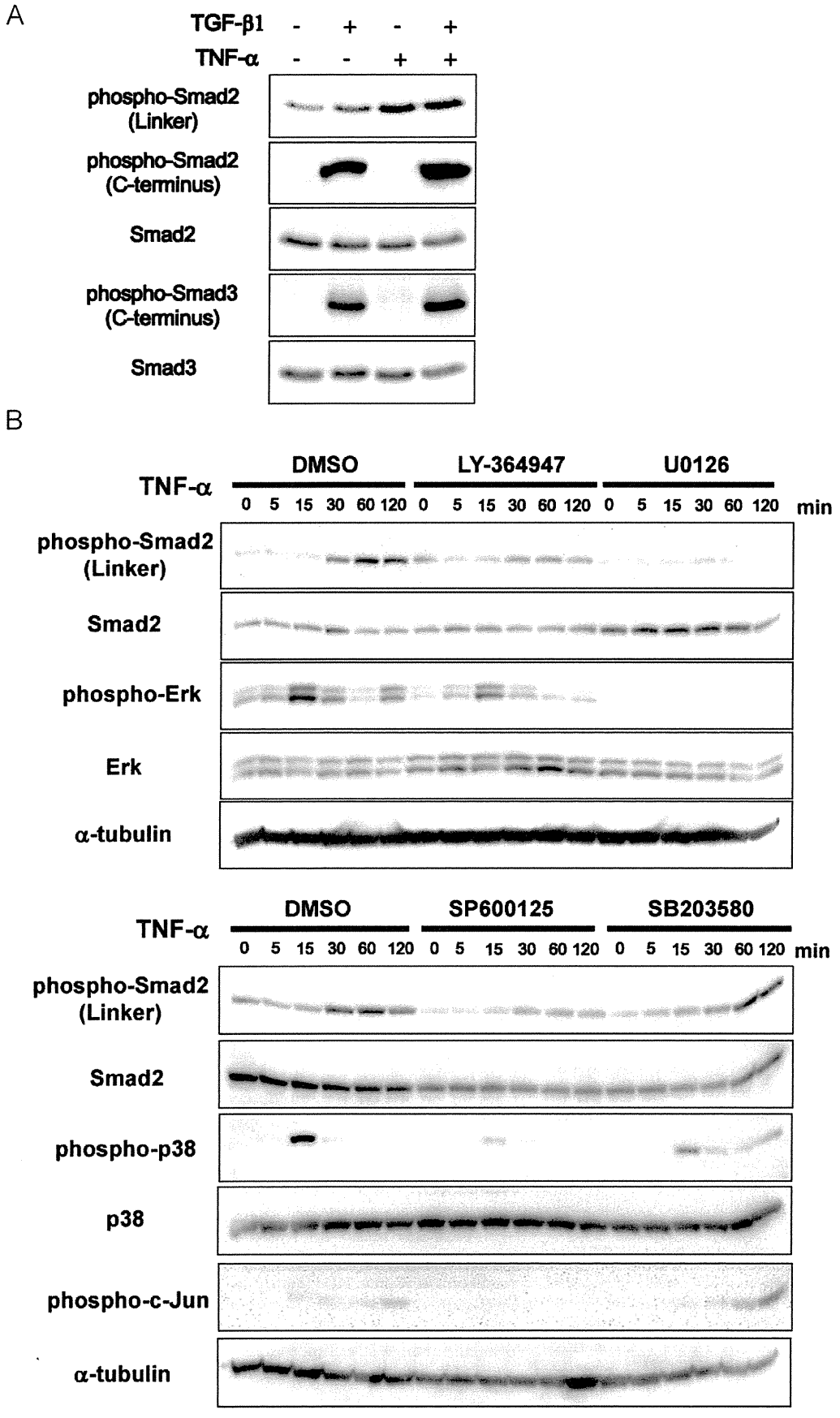
A
TGF-β1 - + - +
TNF-α - - + +
phospho-Smad2 (Linker)
phospho-Smad2 (C-terminus)
Smad2
phospho-Smad3 (C-terminus)
Smad3
B
TNF-α
DMSO
LY-364947
U0126
0 5 15 30 60 120 0 5 15 30 60 120 0 5 15 30 60 120 min
phospho-Smad2 (Linker)
Smad2
phospho-Erk
Erk
α-tubulin
TNF-α
DMSO
SP600125
SB203580
0 5 15 30 60 120 0 5 15 30 60 120 0 5 15 30 60 120 min
phospho-Smad2 (Linker)
Smad2
phospho-p38
p38
phospho-c-Jun
α-tubulin

Figure 3. TNF-α phosphorylates Smad2 linker region via MEK-Erk and JNK pathways. (A) A549 cells were stimulated with TGF-β1 and/or TNF-α for 60 min and immunoblotting was performed for total Smad2, phosphorylated Smad2 (linker region: Ser 245/250/255), phosphorylated Smad2 (C-terminal region: Ser 465/467), total Smad3, phosphorylated Smad3 (C-terminal region: Ser 423/425). (B) A549 cells were pretreated with DMSO or chemical inhibitors (LY-364947, U0126, SP600125 and SB203580) for 60 min, followed by TNF-α stimulation. The cell lysates were collected at the indicated time points, and immunoblotting was performed for Smad2, phosphorylated Smad2 (linker region: Ser 245/250/255), Erk, phosphorylated Erk, p38, phosphorylated p38 and phosphorylated c-Jun. α-tubulin was used as loading control.
doi:10.1371/journal.pone.0056587.g003

EMT is accompanied with enhancement of protease activities that facilitate degradation of basement membrane and extracellular matrices (ECM) surrounding tumor cells, which is critical for tumor invasion/metastasis. To analyze proteolytic activities of matrix metalloproteinases (MMPs) in the cells treated with TGF-β and/or TNF-α, we performed gelatin zymography (Figure 1D). TGF-β enhanced the activity of MMP-2 while TNF-α enhanced that of MMP-9. Notably, costimulation with TGF-β and TNF-α drastically promoted the activities of both MMP-2 and MMP-9, suggesting the synergic effect to enhance MMP activities. In the presence of LY-364947, the effect of TGF-β was clearly inhibited, whereas the effect of TNF-α to enhance MMP-9 activity was still observed albeit to a lesser extent, in the absence of endogenous TGF-β signaling.

To examine the functional aspect of EMT, we performed invasion assay, which utilizes chambers coated with Matrigel, mimicking the basement membrane. TGF-β or TNF-α treatment resulted in modestly increased number of invading cells on the lower face of the chambers, whereas costimulation with TGF-β and TNF-α led to enhanced invasive capacity, in agreement with the above-observed changes (Figure 1E). TGF-β treatment failed to enhance invasive capacity as robust as the changes in EMT markers, suggesting that changes in markers are not directly linked to cell invasiveness. The process of invasion includes enhanced cell motility and proteolytic activities. Together with the results of gelatin zymography, increased invasive capacity in the cells costimulated with TGF-β and TNF-α appeared to be related to enhanced MMP activities.

Taken together, TGF-β-mediated EMT was clearly enhanced by TNF-α as judged by cell morphology, EMT markers, gelatin lysis and cell invasion. TNF-α alone could also induce part of these changes even in the presence of LY-364947, such as N-cadherin upregulation and MMP-9 activation. These observations prompted us to explore the possible crosstalks between TGF-β and TNF-α, and molecular events which regulate EMT in A549 cells.

TGF-β-mediated EMT is Smad-dependent

Smads are the major transducer of TGF-β signaling; Smad2 and Smad3 are phosphorylated by TβR-I, and form complexes with Smad4. These complexes accumulate in the nucleus and regulate transcription of target genes [20]. Besides Smad-mediated transcription, TGF-β activates other signaling cascades, including MAPK (mitogen-activated protein kinase) pathways [21].

To examine whether Smad-mediated signaling is involved in the regulation of EMT in A549 cells, we knocked down endogenous Smad4, which is commonly required for the Smad-mediated transcriptional regulation. Transfection of siRNA effectively silenced Smad4 expression (Figure 2A, left), and further suppressed the expression of Smad-regulated target genes of TGF-β, such as Smad7 and PAI-1 (plasminogen activator inhibitor-1, also known as *SERPINE1*) (Figure 2B). In this setting, TGF-β failed to downregulate E-cadherin as judged by quantitative RT-PCR (Figure 2A, right), suggesting that TGF-β-mediated EMT is mainly regulated by Smad pathway. These effects were further confirmed by immunoblotting. TGF-β failed to downregulate E-cadherin or upregulate N-cadherin efficiently as control siRNA transfected cells when endogenous Smad4 was silenced (Figure 2C).

TNF-α Phosphorylates Smad2 Linker Region

R-Smad and Smad4 contain conserved N-terminal MH1 and C-terminal MH2 domains, flanking the linker segment. Ligand-induced interaction of R-Smads with activated TβR-I results in direct phosphorylation of C-terminal SSXS motif [20], which is the key event of Smad activation. Moreover, other kinase pathways further regulate Smad signaling via phosphorylation of the linker region of R-Smads [21], [22]. Besides NFκB signaling, TNF-α is known to elicit MAPK pathways, which are consisted of three subfamilies, i.e. extracellular signal-regulated kinase (Erk) 1 and 2, p38 MAPK and the c-Jun N-terminal kinase (JNK).

To explore the potential modulation of Smad signaling by TNF-α, we investigated the phosphorylation of the C-terminal or linker regions of R-Smads. TGF-β strongly elicited phosphorylation of Smad2 and Smad3 C-terminal regions whereas TNF-α did not show any effect. On the other hand, TNF-α stimulation led to phosphorylation of the linker region of Smad2, regardless of TGF-β stimulation (Figure 3A).

Next we further sought to elucidate which kinase is involved in TNF-α-mediated phosphorylation of Smad2 linker region, using chemical inhibitors such as LY-364947, U0126, SP600125 and SB203580 (Figure 3B). TNF-α stimulation led to phosphorylation of Erk, p38 and c-Jun, a substrate of JNK. TNF-α stimulation also elicited phosphorylation of the linker of Smad2 in 30–120 min, reaching a peak at 60 min. LY-364947 failed to abolish this effect, showing the effect of TNF-α independent of TβR-I kinase activity. Of the inhibitors tested, TNF-α-mediated Smad2 linker phosphorylation was abrogated by U0126, a MEK inhibitor which could also abolish the phosphorylation of Erk, a downstream substrate of MEK. The JNK inhibitor, SP600125 abolished phosphorylation of c-Jun, a downstream substrate of JNK, and partially inhibited Smad2 linker phosphorylation. The p38 MAPK inhibitor, SB203580 failed to affect Smad2 linker phosphorylation at the concentration shown to be effective in previous reports.

These results suggested that TNF-α elicits phosphorylation of Smad2 linker region, which might modulate Smad-regulated gene transcription [22]. This effect appeared to be largely mediated by MEK-Erk pathway and probably JNK might also play a role, albeit to a lesser extent (Figure 3B).

Microarray Analysis Displays Differential Gene Regulation by TGF-β and TNF-α

To obtain comprehensive insights into the transcriptional changes occurring upon TGF-β and/or TNF-α treatment, gene expression profiling was performed. Total RNA samples were prepared from A549 cells treated with TGF-β and/or TNF-α for 2 h or 24 h, and were further analysed by microarray analysis (Figure 4A). The transcripts induced >1.5-fold or repressed <0.67-fold, including those not annotated, were listed in File S1 and File S2 (the data at 2 h and 24 h, respectively).

For the further analysis, we set the threshold of transcript levels as induced >2.0-fold or repressed <0.5-fold, and excluded unannotated transcripts. Thus we identified genes with altered

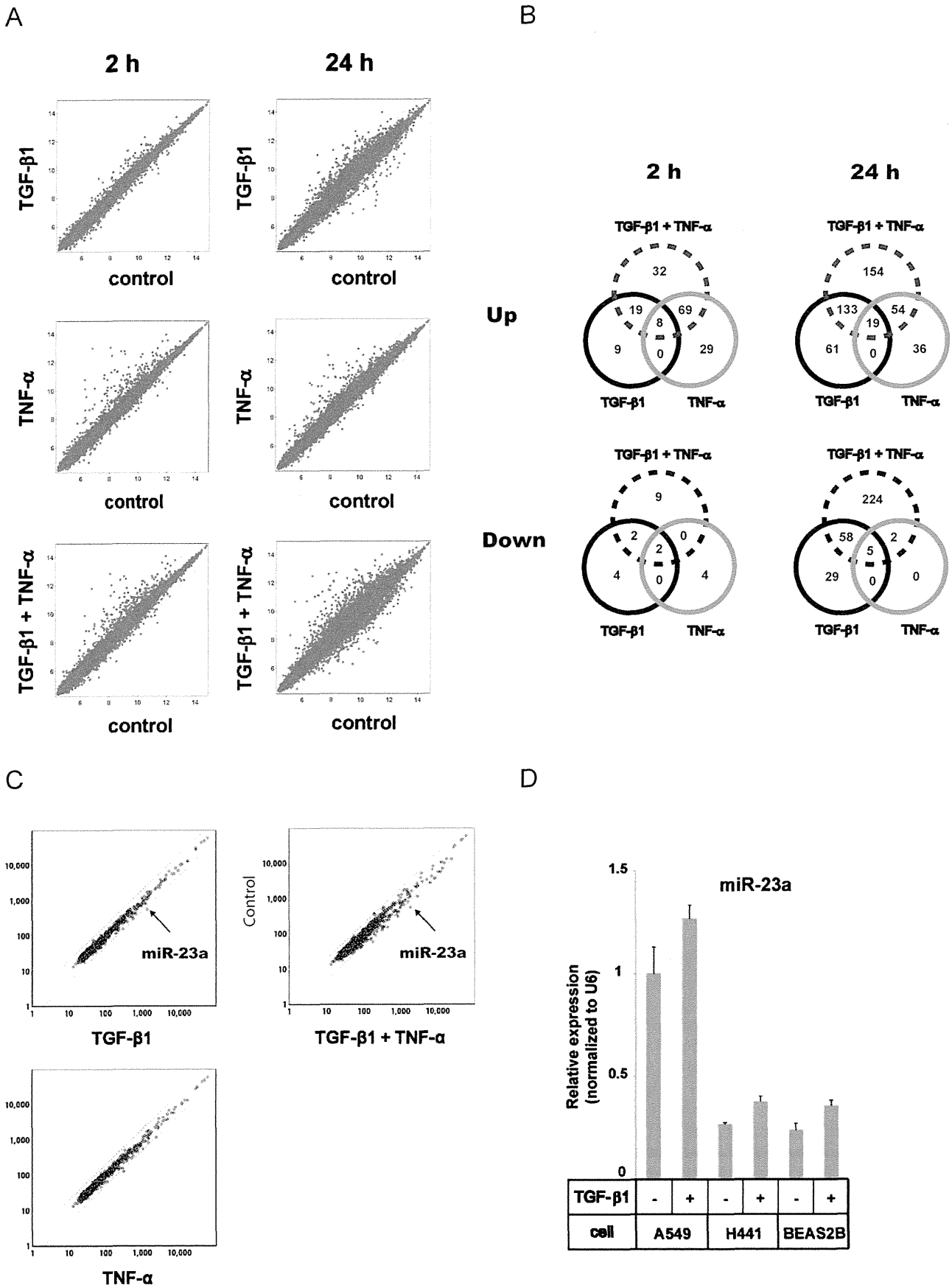
A
2 h
24 h
TGF-β1
TNF-α
TGF-β1 + TNF-α
control
B
2 h
24 h
Up
Down
TGF-β1 + TNF-α
TGF-β1
TNF-α
32
19
69
8
9
29
0
154
133
54
19
61
36
9
2
0
2
4
4
0
224
58
2
5
29
0
C
Control
miR-23a
TGF-β1
TGF-β1 + TNF-α
TNF-α
10,000
1,000
100
10
1
D
miR-23a
Relative expression (normalized to U6)
1.5
1
0.5
0
TGF-β1
cell
A549
H441
BEAS2B

Figure 4. Expression profiling of mRNA and miRNA. (A) Scatter plot representation of the transcripts in the samples treated with TGF-β1 and/or TNF-α for 2 h or 24 h (Y-axis), compared to those of unstimulated control (X-axis). The transcripts are plotted using log2 normalized data. The threshold of transcript levels was set as induced >2.0-fold or repressed <0.5-fold, and is indicated in each scattergram. (B) Venn diagram illustrating the overlap between genes upregulated (Up) or downregulated (Down) by TGF-β1 and/or TNF-α treatment for 2 h or 24 h. The threshold of transcript levels was set as induced >2.0-fold or repressed <0.5-fold. The figures indicate the number of annotated genes. (C) Scatter plot representation of mature miRNAs in the samples treated with TGF-β1 and/or TNF-α for 24 h (X-axis), compared to those of unstimulated control (Y-axis). The threshold of miRNA levels was set as induced >2.0-fold or repressed <0.5-fold, and is indicated in each scattergram. (D) Quantitative RT-PCR for mature miR-23a. A549, H441 and BEAS2B cells were treated with TGF-β1 for 24 h. Expression was normalized to that of U6. Error bars: SD.
doi:10.1371/journal.pone.0056587.g004

expression as compared to unstimulated control, in 3 comparative sets, i.e. TGF-β-stimulated, TNF-α-stimulated and TGF-β/TNF-α-stimulated groups (Figure 4B).

As an overall tendency, TGF-β-regulated and TNF-α-regulated genes were largely exclusive, displaying differential regulation of gene transcription. In addition, upregulated genes were identified much more than those downregulated. The genes induced by TNF-α were more prominent than TGF-β at 2 h, whereas the number of genes upregulated by TGF-β was much greater at 24 h as compared to those at 2 h, or those by TNF-α. At 24 h, there was a fraction of genes which were up- or downregulated by TGF-β and TNF-α costimulation, but not either of them.

Next we employed the published data sets of microarray, which were performed in A549 cells stimulated with TGF-β [23], [24]. Considering induction >2.0-fold as significant, we extracted potential TGF-β target genes commonly induced in three independent studies, i.e. 17 genes at 2h, and 129 genes at 24 h, which are shown in File S3.

Table 1. Upregulated genes by TGF-β1 and/or TNF-α, 2 h after stimulation.

2 h	TGF-β1	TNF-α		TGF-β1+ TNF-α	
Growth factor and receptor	BMBI	INHBA		INHBA	
				HBEGF	
Cytokine and chemokine	IL11	CCL2	IL1A	CCL2	IL1A
		CCL5	IL6	CCL5	IL6
		CCL20	IL8	CCL20	IL8
		CXCL1	CSF2	CXCL1	CSF2
		CXCL2	TNF		TNF
		CXCL3	IL1B		
			IL23A		
Protease and inhibitor				SERPINA3	
SERPINA3					
Regulator of small GTPase	ARL4D	RND1		RND1	
	RND1			GEM	
				RRAD	
Cell adhesion		ICAM1		ICAM1	
		VCAM1			
Others	SMAD7	TNFAIP2	TNFRSF9	TNFAIP2	TNFRSF9
	HEY1	TNFAIP3	TRAF1	TNFAIP3	TRAF1
	ANGPTL4	TNFAIP6	NFKBIA	TNFAIP6	NFKBIA
		SOD2	NFKBIE	SOD2	NFKBIE
		STAT5A		STAT5A	NFKB1
				VDR	

doi:10.1371/journal.pone.0056587.t001

Subsets of Genes Differentially or Cooperatively Regulated by TGF-β and TNF-α

Several transcription factors have been implicated in the transcriptional repression of E-cadherin, including *SNAI1* (Snail), *SNAI2* (Slug), *ZEB1*, *ZEB2* and *TWIST1* [25], [26]. Of these, *SNAI1* was rapidly induced by TGF-β at 2 h whereas TNF-α rather suppressed it, implying the differential mechanisms to regulate EMT. At 24 h, E-cadherin (*CDH1*) was clearly downregulated by TGF-β (0.27-fold) while the suppressive effect of TNF-α was modest (0.78-fold). In accordance, TGF-β and TNF-α upregulated the expression of N-cadherin (*CDH2*) up to 2.32-fold and 1.47-fold, respectively. The synergic effect of TGF-β and TNF-α was also observed with regard to transcriptional regulation of *CDH1* and *CDH2*, consistent with the results in Figure 1.

Furthermore, the genes upregulated more than 3.0-fold at 2 h or 24 h, were subclassified and listed in Table 1 and 2, according to the known functions. As an acute response at 2 h, TNF-α potently induced a number of cytokines/chemokines such as *CCL2* (MCP-1), *CCL5* (RANTES), *CCL20*, *CXCL1*, *CXCL8* (IL8), *IL1A*, *IL1B* and *IL6*. Signaling components of TNF-α-NFκB pathway were also upregulated including *TNF*, *TRAF1*, *NFKB1*, *NFKBIA* and *NFKBIE*. Furthermore, cell adhesion molecules such as *VCAM1* and *ICAM1* were induced. At 2 h after stimulation, TGF-β induced limited number of genes including the known direct targets such as *SMAD7* and *HEY1*. At 24 h, TGF-β stimulation led to enhanced expression of various genes categorized as (i) regulator of small GTPase, (ii) cell adhesion molecule, and (iii) ECM, whereas TNF-α stimulation only showed minor effects on them.

Regulators of small GTPase included guanine nucleotide exchange factors (GEFs) such as *RASGRP1*, *RASGRP3*, *RASGRF2*, *DOCK2* and *DOCK4*, which activate Ras, Rac and Rap1, as well as the members of Rho family GTPases such as *RND1* and *RHOU*. Cell motility and morphological changes are regulated by small GTPases such as Ras, Rac, Cdc42 and Rho families, which can be modulated downstream of TGF-β signaling [27]. Cell adhesion molecules included the members of cadherin such as *CDH4* and *CDH19*, as well as those of integrin family such as *ITGA2*, *ITGA5*, *ITGA11*, *ITGB3* and *ITGB6*. TGF-β stimulation further resulted in highly enhanced expression of the components of ECM such as collagen (*COL1A1*, *COL4A1*, *COL4A2*, *COL5A1*, and *COL5A2*) and laminin (*LAMC2*). As integrins function as receptors for ECM, these expression changes were speculated to modulate bidirectional cell signaling and cellular phenotype [28].

There were two findings regarding the cooperative effects of TGF-β and TNF-α. In the group costimulated with TGF-β and TNF-α, growth factors and their receptors were upregulated including *BMP2*, *INHBA*, *HBEGF*, *FGF5*, *CTGF*, *PDGFB*, *PDGFRA* and *TGFBR1*. Moreover, the expression of proteases and their inhibitors were enhanced, such as MMPs, plasminogen activators (*PLAT* and *PLAU*), and protease inhibitors called as serpins (*SERPINA3*, *SERPINB8*, *SERPINE1* and *SERPINE2*). These proteases and protease inhibitors participate in remodeling of ECM as well as activation/processing of cytokines or growth

Table 2. Upregulated genes by TGF-β and/or TNF-α, 24 h after stimulation.

24 h	TGF-β1		TNF-α		TGF-β1+ TNF-α	
Growth factor and receptor	CTGF		IGFBP1		INHBA	TGFBR1
					PDGFB	PDGFRA
					BMP2	HBEGF
					FGF5	CTGF
Cytokine and chemokine	IL11		CCL2	IL1A	CCL2	IL1A
			CCL5	IL6	CCL5	IL6
			CCL20	IL8	CCL20	IL8
			CXCL1	EBI3 (IL27)		IL11
						IL32
						IL33
Protease and inhibitor	MMP2		MMP1		MMP1	SERPINA3
	ADAM19		SERPINA3		MMP2	SERPINB8
	SERPINE1		SERPINB8		MMP9	SERPINE1
					PLAT	SERPINE2
					PLAU	ADAM19
Regulator of small GTPase	RASGRP1	RHOU			RASGRP1	RHOU
	RASGRP3	DOCK2			RASGRP3	DOCK4
	RASGRF2	DOCK4			RASGRF2	RND1
Cell adhesion	ITGA11	CDH4	ICAM1		ITGA2	CDH4
	ITGB6	CDH19			ITGA5	CDH19
		ESAM			ITGB3	ICAM1
						DSC2
Extracellular matrix	COL4A1	PODXL	LAMC2		COL4A1	SPOCK1
	LAMC2	HAPLN3			LAMB3	PODXL
	SPOCK1				LAMC2	HAPLN3
Others	TNFAIP6	ANGPTL4	TNFAIP3	VDR	TNFAIP3	ANGPTL4
	LOX	ABLIM3	TNFRSF9		TNFAIP6	ABLIM3
		SLN	NFKB1		TNFRSF9	SLN
		TAGLN	NFKB2		NFKB1	VDR
		MYOCD			NFKB2	FERMT1

doi:10.1371/journal.pone.0056587.t002

factors. Thus TGF-β and TNF-α might cooperatively alter the extracellular milieu surrounding cancer cells structurally as well as functionally. TNF-α and TGF-β also upregulated genes involved in hyaluronan remodeling, such as *HAS2*, *HAS3* and *HAPLN3*, which might have a role in EMT regulation through hyarulonan-CD44 interaction [29]. Strong induction of *PODXL* (podocalyxin) following TGF-β treatment was also observed as reported previously [30].

MicroRNA Array Analysis Reveals miR-23a as a Target of TGF-β

Noncoding microRNAs (miRNAs) are also critical components of cellular signaling implicated in the regulation of EMT. In the list of microarray data, we noted distinct populations of genes which were suppressed by TGF-β and TNF-α, and we hypothesized that their expression could be regulated by miRNAs. In search of miRNAs induced by TGF-β and TNF-α, we performed miRNA array analysis (Figure 4C). The normalized data of TGF-β-stimulated, TNF-α-stimulated and TGF-β/TNF-α-stimulated groups were listed in File S4. Mature miRNAs induced >2.0-fold included miR-23a in the TGF-β-stimulated sample (2.61-fold), while any miRNA with >2.0-fold induction was not noted in the TNF-α-stimulated sample. Costimulation with TGF-β and TNF-α induced miR-23a (3.32-fold), miR-720, miR-4275 and miR-4285.

Next we validated the induction of miR-23a by TGF-β in lung cancer/epithelial cell lines, i.e. A549 and H441 lung cancer cells as well as BEAS2B transformed bronchial epithelial cells. In all these cell lines, TGF-β could induce mature miR-23a as confirmed by quantitative RT-PCR (Figure 4D).

Integrated Analysis of mRNA and miRNA Arrays Reveals Potential Targets Regulated by TGF-β and miR-23a

We proceeded to explore the potential participation of miR-23a in the regulation of TGF-β-elicited EMT, and searched for target genes which could be regulated by miR-23a.

It has been demonstrated that miR-23a promotes invasive capacity of colon cancer cells [31], and miR-23a targets E-cadherin to modulated EMT in lung cancer cells [32]. However, miR-23a inhibition could not modulate TGF-β-elicited EMT in A549 cells (Figure S1). Additionally, transfection of synthetic precursor miR-23a (pre-miR-23a) failed to alter the expression of

A

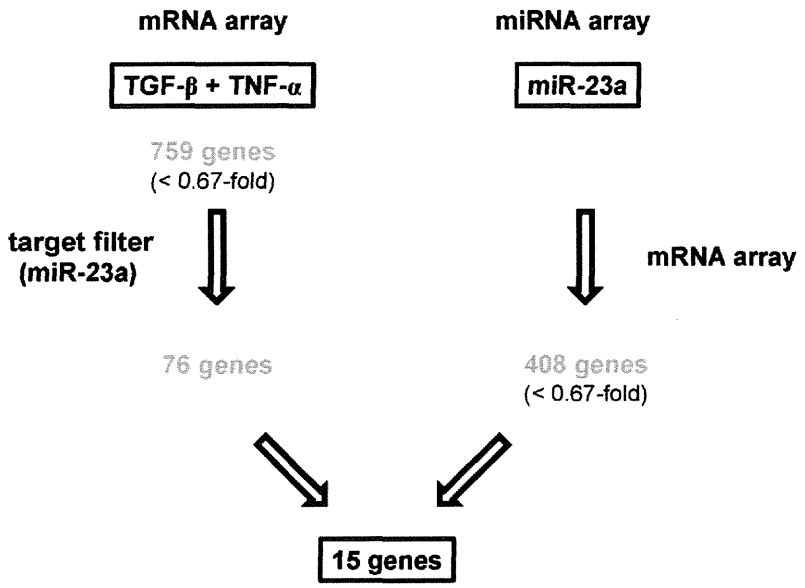

B

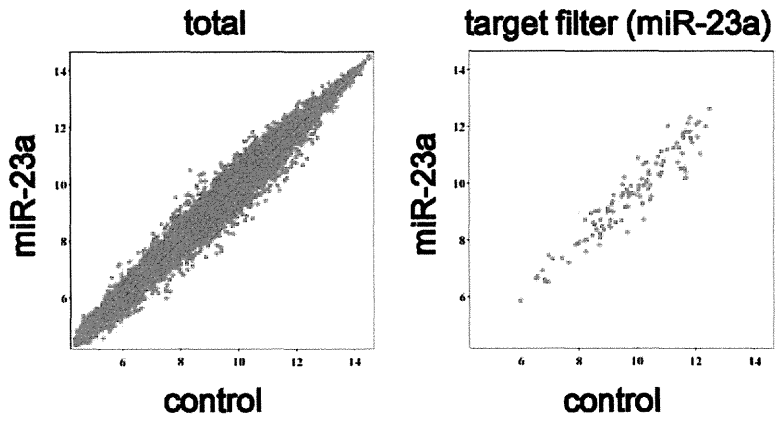

C

Genbank ID	Gene symbol
AY358712	DHRS11
CR542122	HMGN2
BC008376	CXCL5
BC010918	NTS
AK295434	POLR3G
BC072433	SNRPE
AF032862	HMMR
AB281187	DEPDC1
AK290193	BTN3A1
BC089410	IL6R
BC064600|AF516710	CCDC111|MLF1IP
BC015514	TFPI
BC100019	HMGB2
AK304347	ERI2
AK291842	PLEKHA2

Figure 5. Putative targets of TGF-β-induced miR-23a. (A) Schematic description of integrated analysis of mRNA and miRNA arrays. Gene expression signature in the cells treated with TGF-β1 and TNF-α revealed 759 annotated genes downregulated <0.67-fold. Out of them, the target filter program listed 76 genes as putative miR-23a targets. Transfection of synthetic pre-miR-23a in A549 cells identified 408 genes downregulated

<0.67-fold. There were 15 genes shared in these two groups. (B) Scatter plot representation of the transcripts in A549 cells transfected with control (X-axis) or synthetic pre-miR-23a (Y-axis) for 48 h. The transcripts are plotted using log2 normalized data. The threshold of transcript levels was set as induced >2.0-fold or repressed <0.5-fold, and is indicated in each scattergram. Plots of total transcripts (right), and those selected by the target filter program (right), are presented. (C) The list of 15 genes identified by integrated analyses.
doi:10.1371/journal.pone.0056587.g005

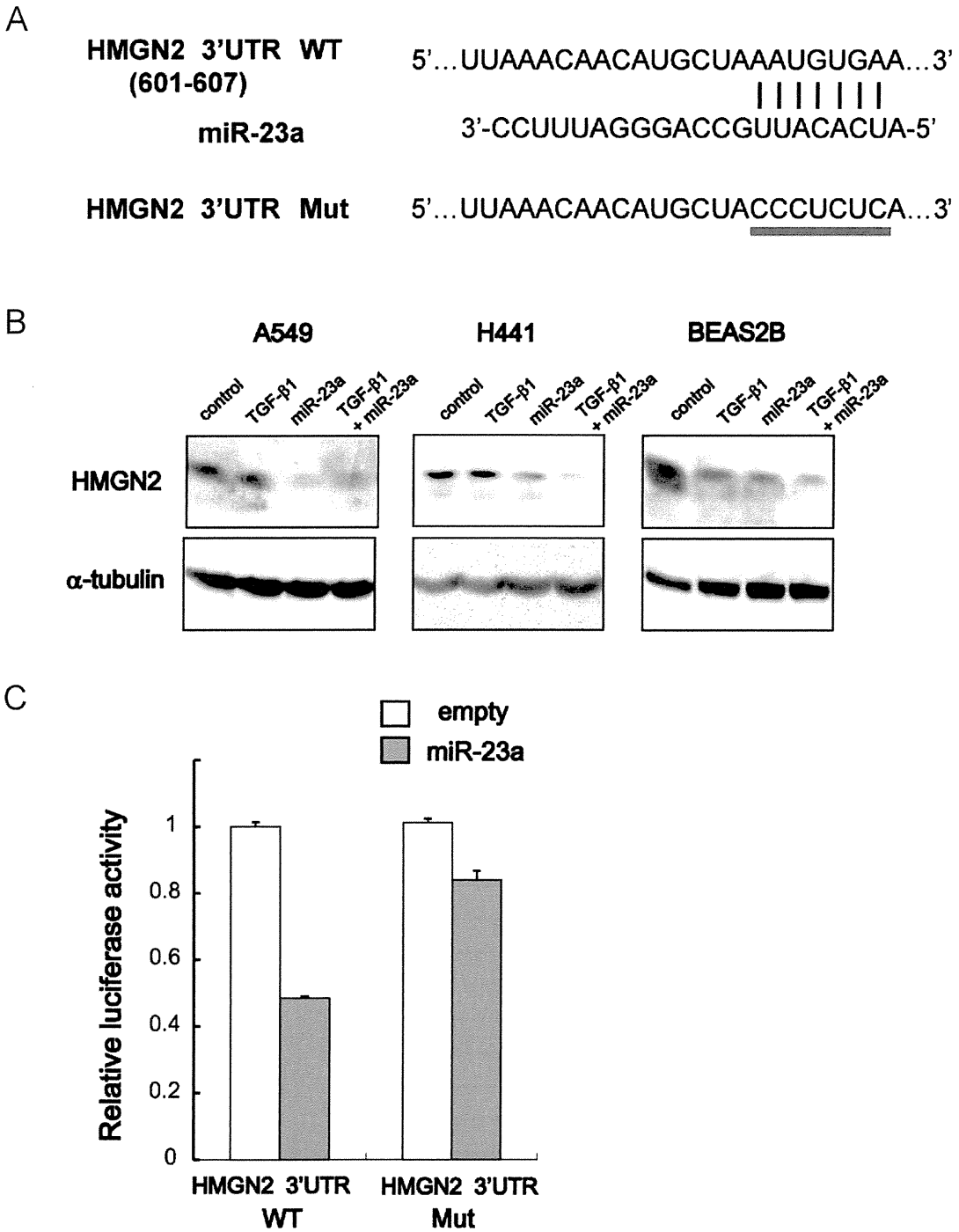

Figure 6. HMGN2 is regulated by miR-23a. (A) Putative miR-23a binding sequence in the 3'UTR of human HMGN2 mRNA (WT: wild-type). The underlined sequence shows the nucleotides generated by mutagenesis to abolish the binding of miR-23a (Mut: mutant). (B) Immunoblotting for HMGN2 in A549, H441 and BEAS2B cells transfected with control or synthetic pre-miR-23a for 48 h, followed by TGF-β1 stimulation for additional 48 h. α-tubulin was used as loading control. (C) HEK293T cells were transfected with luciferase reporters containing the HMGN2 3'UTR with wild-type or mutated target site as shown in Fig. 6A, along with empty or pri-miR-23a expression vector. Luciferase assay was performed 48 h after transfection.
doi:10.1371/journal.pone.0056587.g006

E-cadherin or N-cadherin (Figure S1). Thus miR-23a did not appear to play a role in our model of EMT.

Next we explored to identify potential miR-23a targets. Utilizing the miRNA target filter in IPA analysis, 76 genes were extracted out of 759 genes which were downregulated <0.67-fold by TGF-β and TNF-α (Figure 5A). To further validate target genes potentially regulated by miR-23a, we performed gene expression profiling in the cells transfected with pre-miR-23a or negative control, which yielded 408 genes downregulated <0.67-fold by pre-miR-23a transfection (Figure 5B). Combining these array results, 15 genes were extracted as targets of TGF-β/TNF-α as well as miR-23a (Figure 5A and 5C).

Out of the 15 genes, we selected *HMGN2* (high motility group nucleosomal 2, also known as *HMG-17*) for further analyses, since it is implicated in cellular differentiation and cancer [33], [34]. The putative miR-23a binding sequence in the 3′UTR of human HMGN2 transcript was identified by Targetscan (Figure 6A). To confirm miR-23a-mediated suppression of HMGN2, immunoblotting for HMGN2 was performed after TGF-β stimulation and/or pre-miR-23a transfection (Figure 6B). TGF-β downregulated HMGN2 in BEAS2B cells whereas it did not affect HMGN2 expression in A549 or H441 cells at protein level. On the other hand, pre-miR-23a transfection clearly led to suppression of HMGN2 in all these cell lines.

To investigate the direct regulation of HMGN2 by miR-23a, wild-type 3′UTR of HMGN2 mRNA was subcloned downstream of the luciferase reporter. We also constructed the reporter vector with mutations in the putative miR-23a binding site (Figure 6A). As expected, luciferase activity was markedly reduced when the miR-23a expression vector was cotransfected, whereas the miR-23a-induced decrease in luciferase activity was abolished for the mutant reporter vector (Figure 6C).

Discussion

The cooperative action of TGF-β and TNF-α on EMT attracts increasing attention since it reflects the cancer microenvironment infiltrated with inflammatory cells, and provides a model where inflammatory signals enhance tumor progression [13], [14], [15]. This idea is also supported by the observation that activated macrophages can enhance TGF-β-mediated EMT [35], [36]. Recently it has been also reported that tumor cells treated with TGF-β and TNF-α generates a population of stem cells, further evoking attention on their possible crosstalks [37].

The present study demonstrated that TGF-β and TNF-α synergically induces EMT in A549 lung cancer cells. Their effect was mostly dependent on Smad pathway, and TNF-α could induce phosphorylation of Smad2 linker region, suggesting the possible modulation of Smad-regulated gene transcription. Gene expression signature revealed cohorts of genes differentially or cooperatively regulated by TGF-β and TNF-α. Furthermore, miRNA array analysis identified miR-23a, as a target of TGF-β. Integrated analysis of mRNA and miRNA expression profiles, combined with in silico screening, provided a list of genes, possibly regulated via miR-23a. We further validated miR-23a-mediated regulation of HMGN2.

The miR-23a is transcribed from the miR-23a~27a~24-2 cluster on chromosome 19p13, followed by cleavage to yield mature miR-23a. The miR-23b~27b~24-1 cluster is its paralog on chromosome 9q22, and mature miR-23a differs by just one nucleotide compared to miR-24, suggesting their overlapping targets [38]. These three miRNAs of this cluster are derived from a single primary transcript, but the levels of each can vary because of post-transcriptional processing [38], [39].

Upregulation of miR-23a has been documented in a variety of human cancers including gastric cancer, glioblastoma, breast cancer, and pancreatic cancer [40]. Consistent with our observation, it has been shown that miR-23a or miR-24 can be induced by TGF-β in keratinocytes and hepatocellular carcinoma cells [41], [42]. Furthermore, upregulation of miR-23a in association with TGF-β signaling has been reported in non-small cell lung cancer cells [32]. In this study, we could not find any effect of miR-23a on EMT markers, though it does not exclude the possibility that miR-23a might have an impact on molecular events accompanying EMT. Further studies are warranted to clarify the exact role of miR-23a in lung cancer cells undergoing EMT.

Out of 15 genes chosen as putative miR-23a targets by integrated analyses, IL-6 receptor (*IL6R*) has been experimentally validated [43]. In addition to this previous report, we have for the first time, validated HMGN2 as a direct target of miR-23a, in the current study. HMGN2 regulates transcription via alteration of chromatin structure through interfering with the binding of linker histone H1 to the nucleosome. Recently, microarray analyses revealed genes potentially regulated by HMGN2 in A549 cells, which suggested HMGN2-mediated modulation of diverse cell signals [44]. Thus HMGN2 has been implicated as a downstream effector of miR-23a.

In conclusion, integrated analyses of gene and miRNA expression profiling delineated cooperative and differential action of TGF-β and TNF-α, and unraveled potential roles of miRNAs. We have shown that miR-23a was induced by TGF-β, and identified HMGN2 as a target of miR-23a. Our findings shed light on the complexity of molecular events accompanying EMT, elicited by TGF-β and TNF-α.

Supporting Information

Figure S1 Immunoblotting for E-cadherin and N-cadherin in A549 cells transfected with control versus synthetic pre-miR-23a, or control versus miR-23a inhibitor for 48 h, followed by TGF-β1 stimulation for additional 48 h. α-tubulin was used as loading control.
(EPS)

Table S1 Primers used for quantitative RT-PCR in this study.
(EPS)

Table S2 Primers used for the construction of 3′UTR reporter vector and pri-miRNA expression vector.
(EPS)

File S1 The transcripts at 2 h induced >1.5-fold or repressed <0.67-fold, including those not annotated.
(XLSX)

File S2 The transcripts at 24 h induced >1.5-fold or repressed <0.67-fold, including those not annotated.
(XLSX)

File S3 Integrated analysis with the published data sets of microarray, which were performed in A549 cells stimulated with TGF-β. Considering induction >2.0-fold as significant, we extracted potential TGF-β target genes commonly induced in three independent studies, i.e. 17 genes at 2 h, and 129 genes at 24 h.
(XLSX)

File S4 MicroRNA array analysis. The normalized data of TGF-β-stimulated, TNF-α-stimulated and TGF-β/TNF-α-stimulated groups.
(XLSX)